

Keggin Based Self Assembled Mesoporous Materials for the Capture of Selective Guest Molecules

Kesar Tandekar,^a Anjali Tripathi,^a Muvva D. Prasad^b and Sabbani Supriya^{a*}

Table of Contents:

Section S1	Physical Measurements	2
Section S2	Materials and Synthesis Procedures	2-3
Section S3	Fourier Transform Infrared (FT-IR) Spectroscopic Analysis	3-4
Section S4	Powder X-ray Diffraction (PXRD) Studies	4-5
Section S5	Energy Dispersive X-ray (EDX) Spectroscopy	5-6
Section S6	Field Emission Scanning Electron Microscopy (FESEM)	7
Section S7	Transmission Electron Microscopy (TEM)	8
Section S8	Thermogravimetric Analysis (TGA)	9-14
Section S9	N ₂ Sorption Studies	15-16
Section S10	Iodine adsorption by mesoporous compounds 1-9	17-22
Section S11	Adsorption of CS ₂ by mesoporous compound 1	22-23
Section S12	Surface potential measurements	24 - 25
Section S13	Control experiments of iodine adsorption by phosphonium cations	26 - 27

Section S1. Physical Measurements

Fourier Transform Infrared spectra (FT-IR) of the solid samples were recorded at room temperature in the range of 400-4000 cm^{-1} on a Shimadzu FT-IR spectrophotometer. Room temperature powder X-ray diffraction patterns for the solid samples were measured on a Rigaku Powder X-ray diffractometer, Miniflex-600 equipped with a Cu $K\alpha$ radiation source ($\lambda = 1.540 \text{ \AA}$) operating in Bragg-Brentano geometry. The solution state UV-visible spectroscopic experiments were conducted on a Shimadzu UV 2600 UV-vis spectrophotometer in the wavelength range of 200-800 nm. The Field Emission Scanning Electron Microscope (FESEM) imaging was carried out on a Carl Zeiss model Ultra 55 microscope: EDX spectra were recorded using Oxford Instruments X-Max^N SDD (50 mm^2) systems and INca analysis software. The images were recorded for solid sample deposited as a very fine film on the surface of carbon tape. The Transmission Electron Microscope (TEM) images were recorded on a JEOL 2100F instrument. The TEM sample was prepared by dispersion of the solid sample in water followed by sonication for 30 minutes. The sonicated suspension was coated on the TEM copper grid through drop casting followed by drying at room temperature. The TGA data was recorded on a Mettler Toledo TGA 1 instrument for the temperature range of 25°-700°C at the rate of 5°C min^{-1} under an inert flow of dry N_2 gas (flow rate 20 $\text{cm}^3\text{min}^{-1}$). The room temperature NMR spectra were recorded on a Bruker Avance III (500 MHz). The NMR data was recorded in d_6 -DMSO solvent. Chemical shifts are indicated as δ values with respect to TMS which is used as an internal standard. The specific surface area measurements were performed by Brunauer-Emmett-Teller (BET) method using Quantachrome Autosorb-ICTCD analyzer.

Section S2. Materials and Synthesis Procedures

All the chemicals (phosphomolybdic acid, silicomolybdic acid, phosphotungstic acid, silicotungstic acid, tetraphenylphosphonium bromide, methyltriphenyl phosphonium bromide, ethyltriphenylphosphonium bromide, iodine, carbon disulfide) were of reagent grade, received from commercial sources and used as received. Deionized water was used throughout the synthesis.

S2.1. Synthesis of Compounds 1-9

An aqueous solution of Keggin (0.42 mmol in 75 mL) was prepared. To it, 25 mL aqueous-methanolic (4:1 v/v) or aqueous solution of phosphonium cation (RPPH_3 ; R = Me, Et, Ph) (3.5 mmol) was added. The obtained suspension was refluxed for two hours at 100°C . The resultant polycrystalline precipitate was washed with water and vacuum dried. Yield: 85-90 %.

Section S3. Fourier Transform Infrared (FT-IR) Spectroscopic Analysis

S3.1. The IR spectra of the phosphonium cations RPPH_3Br used in the synthesis of the porous self-assembled structures are given in Figure 1.

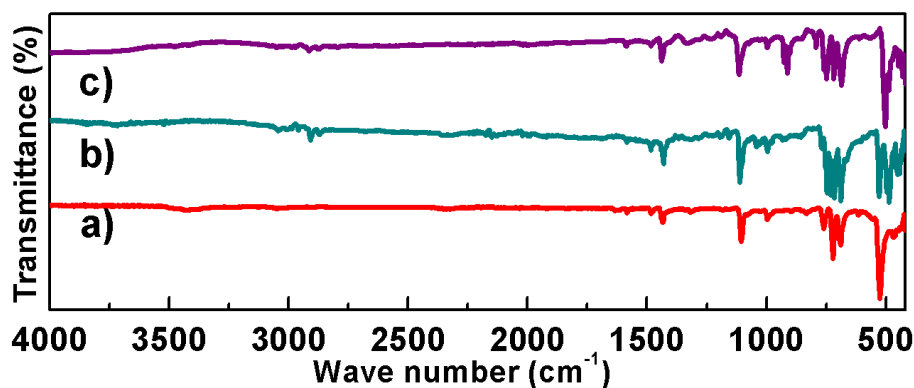


Fig. S1a. IR spectra for a) PPh_4Br ; b) EtPPH_3Br ; c) MePPH_3Br .

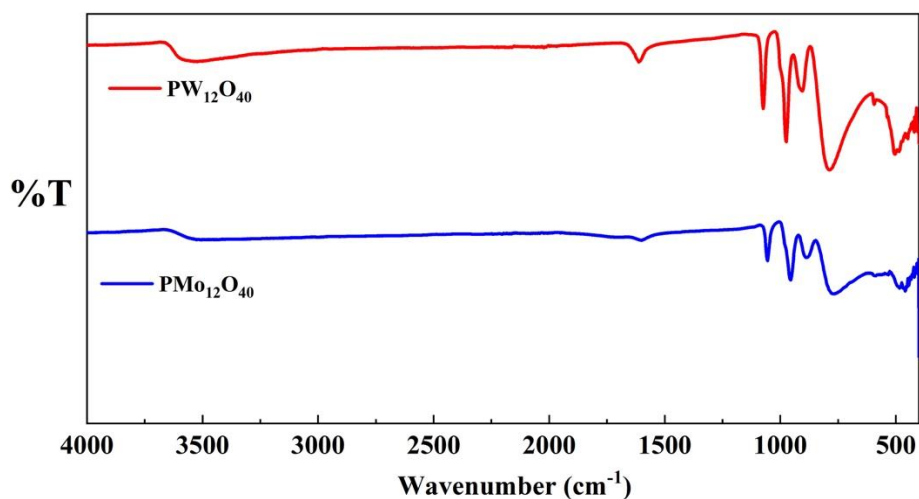


Fig. S1b. IR spectra of phosphotungstic acid (red line) and phosphomolybdic acid (blue line).

S3.2. Compounds **1-9** were applied for the adsorption of I_2 . The adsorbed iodine was then extracted in hexane. The IR data for the porous materials were recorded post the processes of adsorption and desorption of iodine which showed that the compounds did not disintegrate during either of the processes (Figure S2a-b).

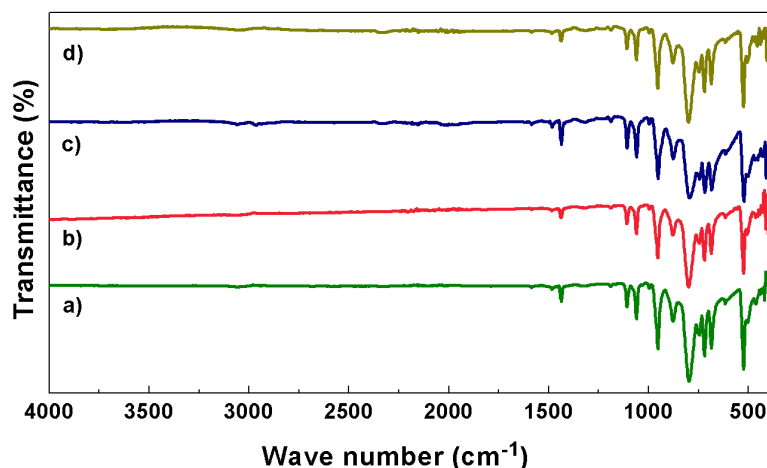


Fig. S2a Comparative IR spectra for a) Compound **1**; b) Compound **1** after I_2 adsorption; c) Regenerated compound **1** after I_2 desorption; d) Regenerated compound **1** after five adsorption cycles of I_2 .

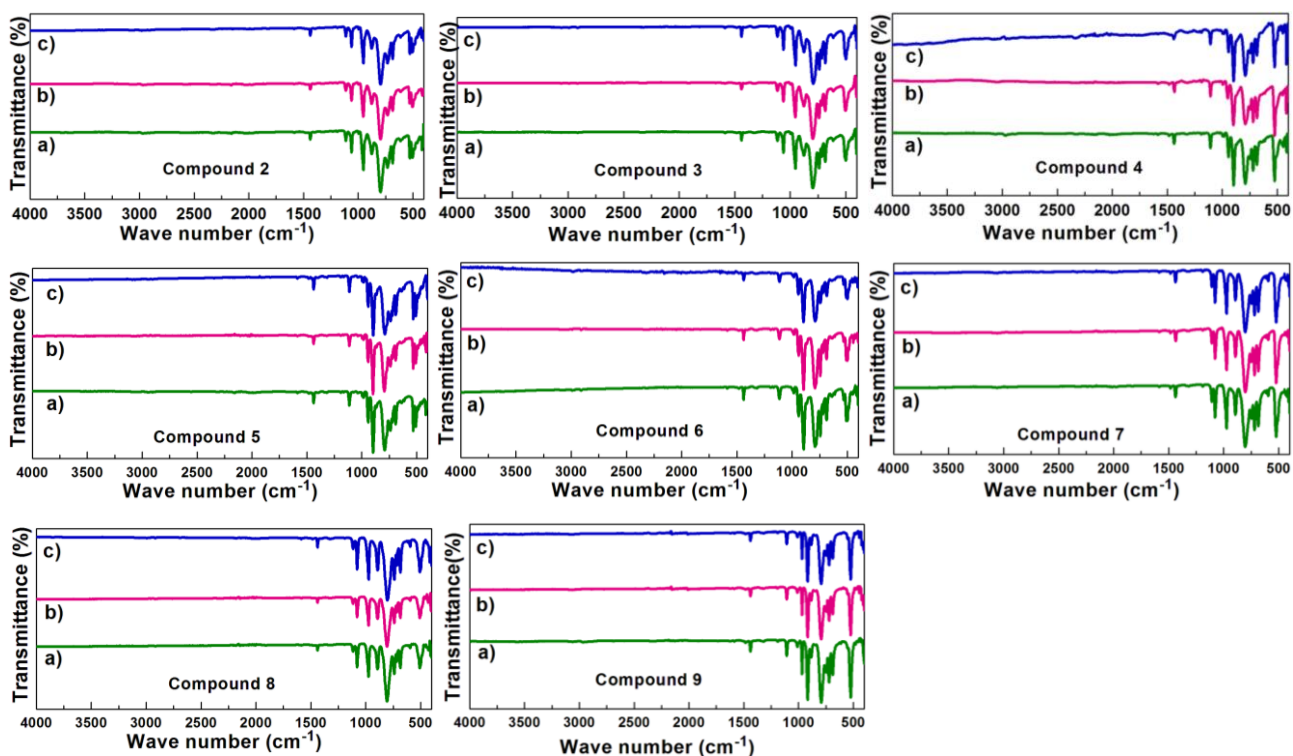


Fig. S2b Comparative IR plots for compounds **2-9** a) as synthesized mesoporous compound b) mesoporous compound after I_2 adsorption c) regenerated compound after I_2 desorption.

Section S4. Powder X-Ray Diffraction (PXRD) Studies

S4.1. The PXRD patterns for the phosphonium cations RPPH_3Br used in the synthesis of the porous materials **1-9** are given in **Figure S3**.

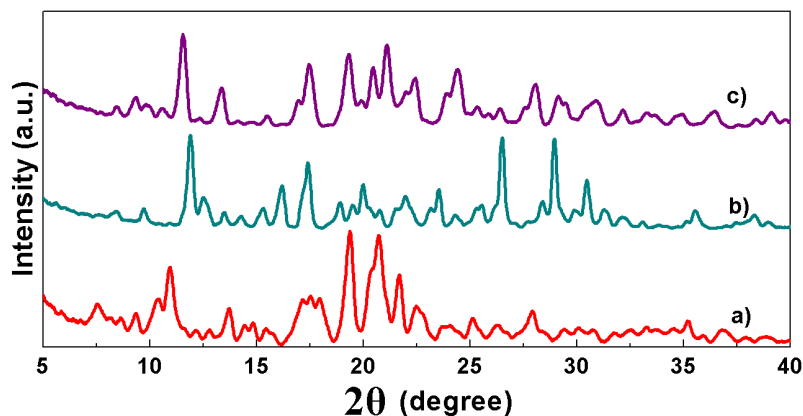


Fig. S3 PXRD plot for a) PPh_4Br ; b) EtPPh_3Br ; c) MePPh_3Br .

S4.2. The PXRD plots obtained for compound **1** post the cycle of adsorption and desorption of I_2 showed no phase change or structure disintegration for the porous material (Fig. S4).

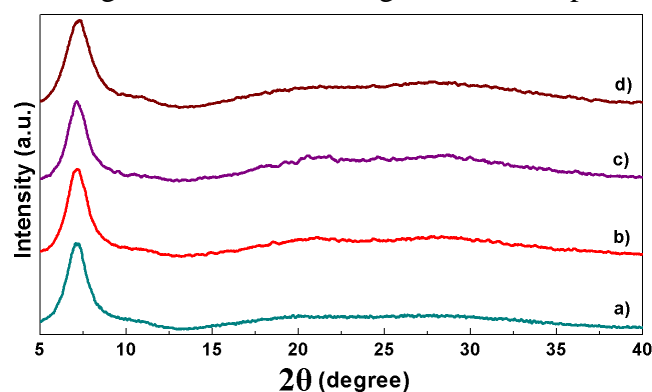


Fig. S4 Comparative PXRD plots for a) Compound **1**; b) Compound **1** exposed to I_2 ; c) Regenerated compound **1** after one cycle of I_2 extraction in hexane; d) Regenerated compound **1** after five cycles of I_2 extraction in hexane.

S4.3. The PXRD plots obtained for compound **1** post the cycle of adsorption and desorption of CS₂ showed no phase change or structure disintegration for the porous material (Fig. S5).

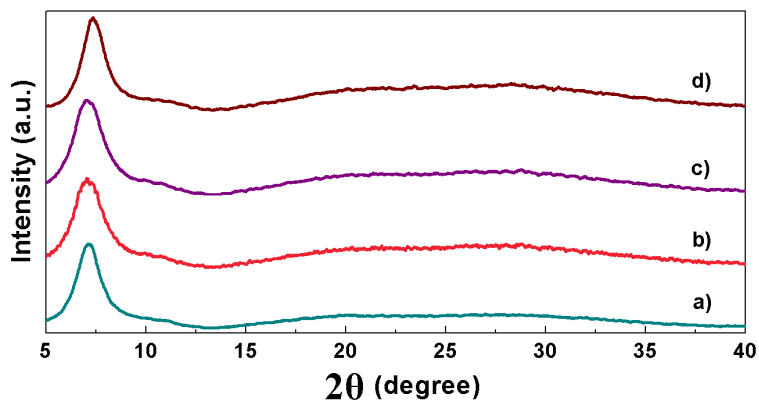


Fig. S5 Comparative PXRD spectra for a) Compound **1**; b) Compound **1** exposed to CS₂; c) Regenerated compound **1** after one cycle of CS₂ extraction in methanol; d) Regenerated compound **1** after five cycles of CS₂ extraction in methanol.

Section S5. Energy Dispersive X-Ray (EDX) Spectroscopy

The FESEM-EDX data for compounds **1-9** shows uniform distribution of carbon, phosphorous, molybdenum (or tungsten) on the surface of porous materials (Fig. S6).

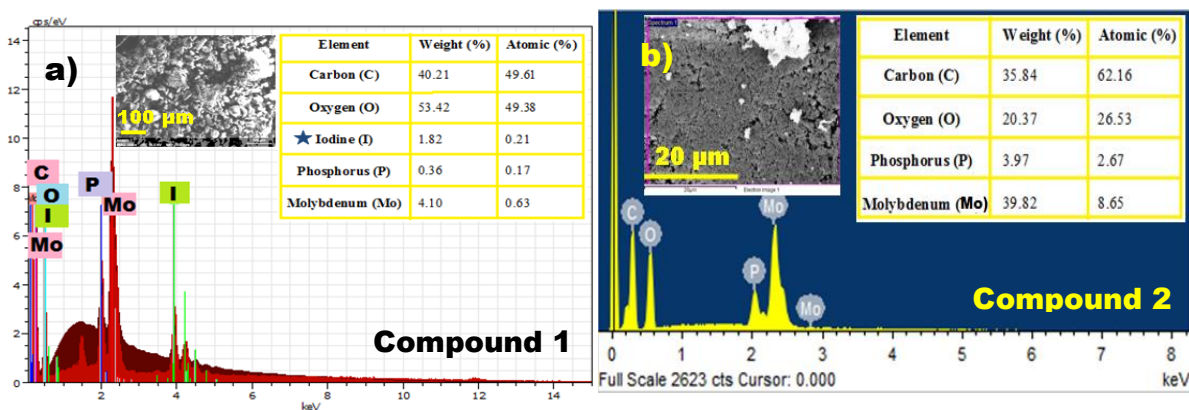




Fig. S6. a-i) FESEM-EDX for mesoporous compounds 1-9. The sample surface shows the presence of C, O, P (and/or Si) and Mo (or W) in the respective compounds. The weight and atomic percentages are summarized in tabular form.

Section S6. Field Emission Scanning Electron Microscopy (FESEM)

The FESEM images for compounds **1-9** show the presence of coral aggregates along with inner channels and cavities (Fig. S7).

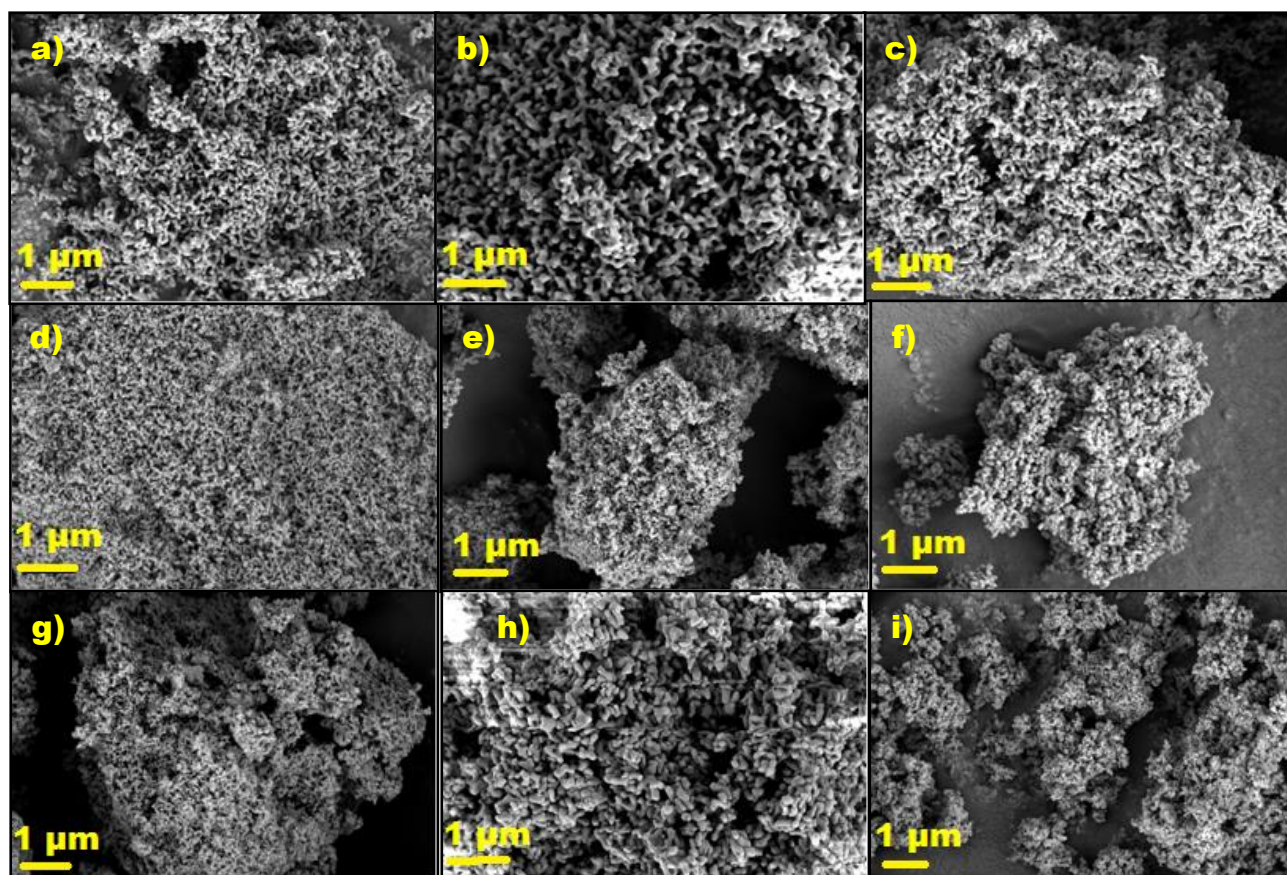


Fig. S7 FESEM images for a) Compound **1**; b) Compound **2**; c) Compound **3**; d) Compound **4**; e) Compound **5**; f) Compound **6**; g) Compound **7**; h) Compound **8**; i) Compound **9**.

Section S7. Transmission Electron Microscopy (TEM)

The TEM images for compounds **1-9** show the presence of spherical (slightly elongated) aggregates, formed due to the arrangement of the phosphonium cations on the surface of the Keggin ions, which are held together by electrostatic interactions (Fig. S8).

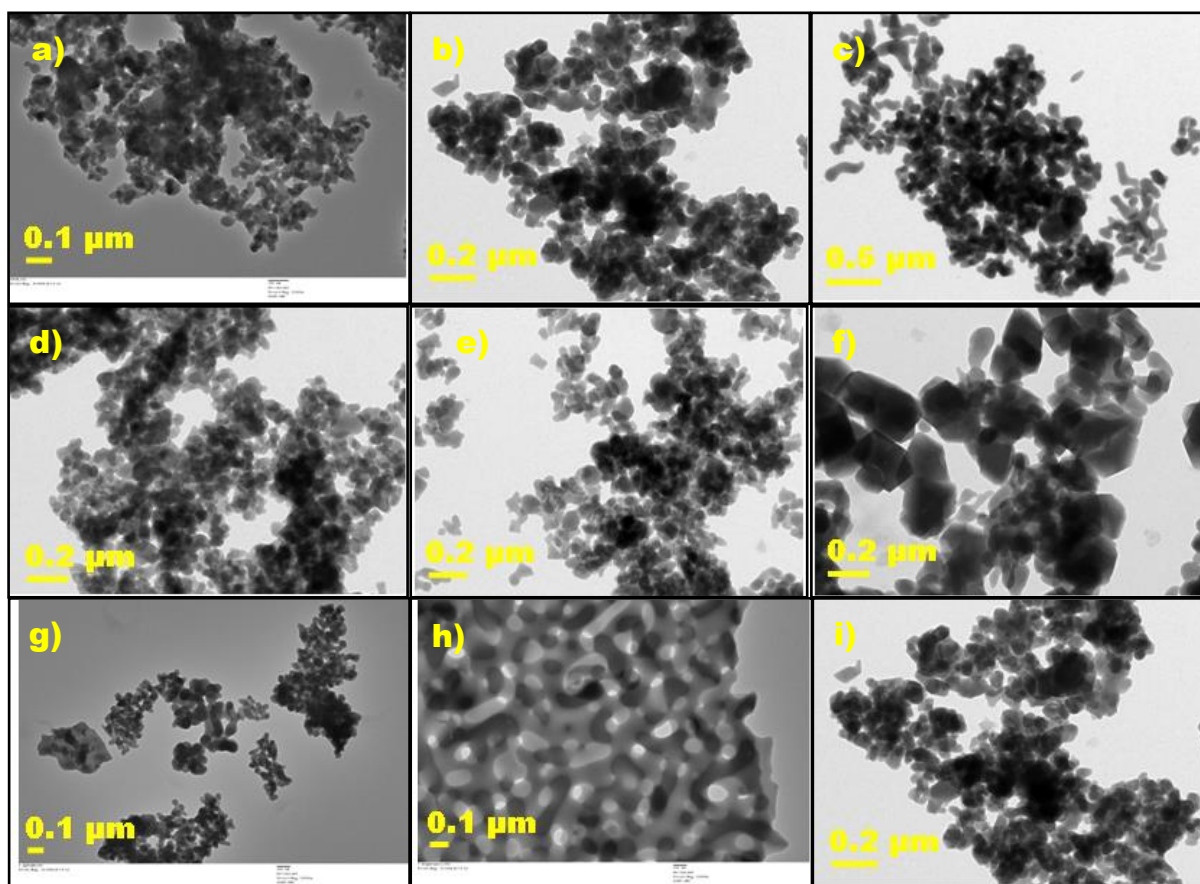


Fig. S8 TEM images for a) Compound **1**; b) Compound **2**; c) Compound **3**; d) Compound **4**; e) Compound **5**; f) Compound **6**; g) Compound **7**; h) Compound **8**; i) Compound **9**.

Section S8. Thermogravimetric Analysis (TGA)

S8.1. The stability of the Keggin-based hybrid materials **1-9** was examined between temperature range of 25°-800°C. As per the thermograms, shown in Fig. S9 and Figures S10a-i, the mesoporous compounds display high thermal stability showing structural disintegration only beyond 300°C.

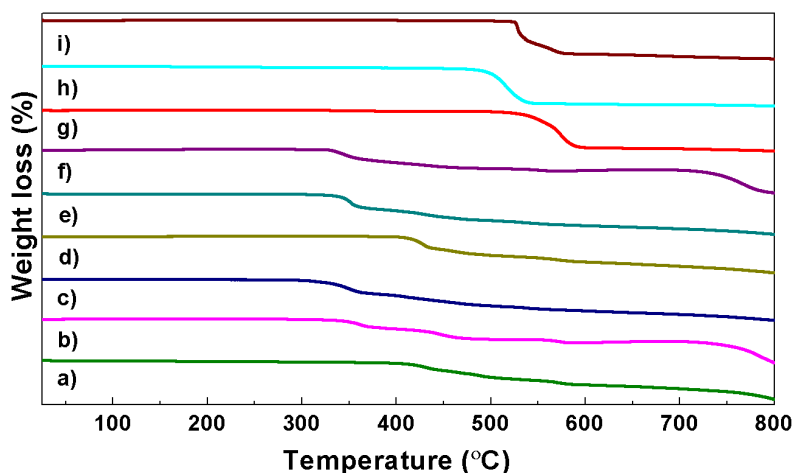


Fig. S9 Thermograms in temperature range of 25°-800°C for a) compound **1**; b) compound **2**; c) compound **3**; d) compound **4**; e) compound **5**; f) compound **6**; g) compound **7**; h) compound **8**; i) compound **9**.

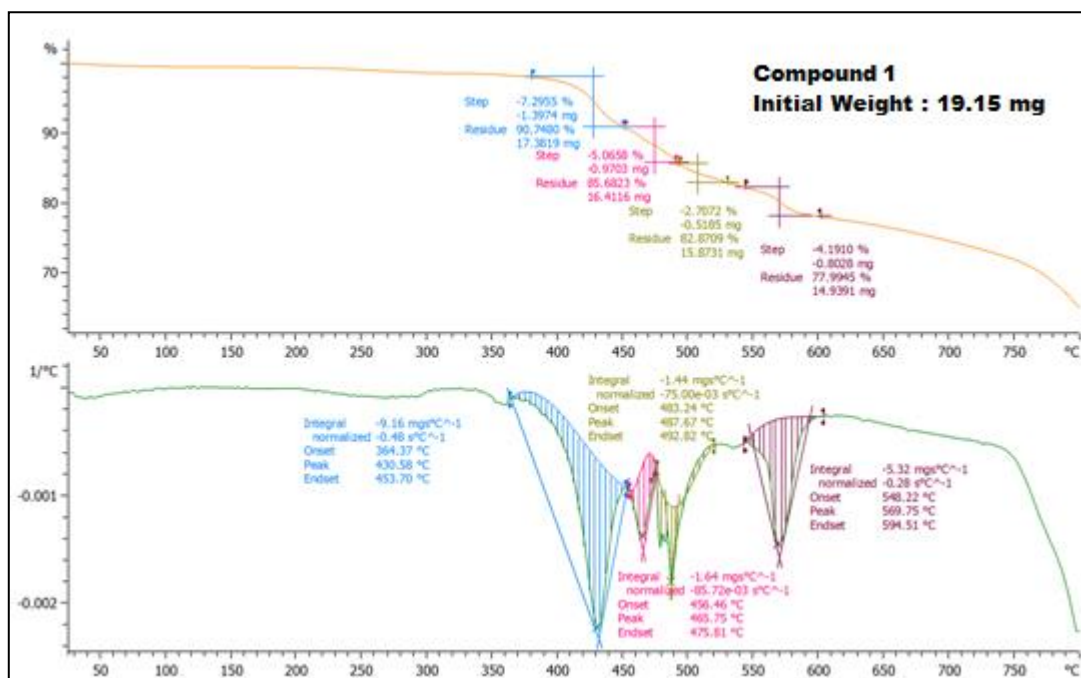


Fig. S10a Thermal analysis plot for compound **1**.

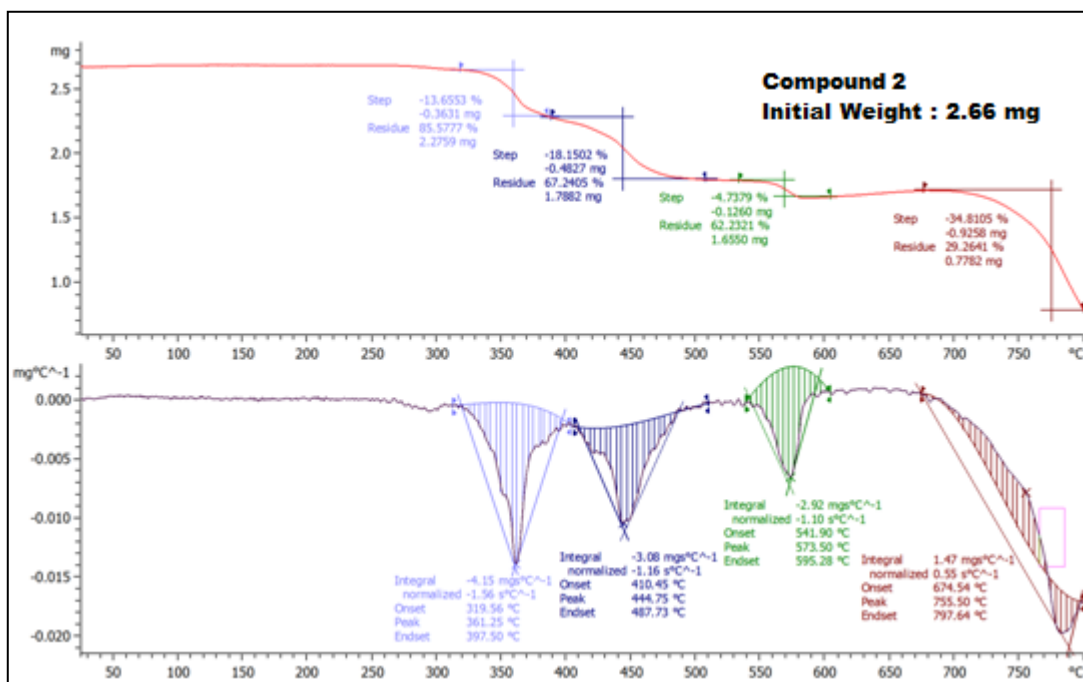


Fig. S10b Thermal analysis plot for compound 2.

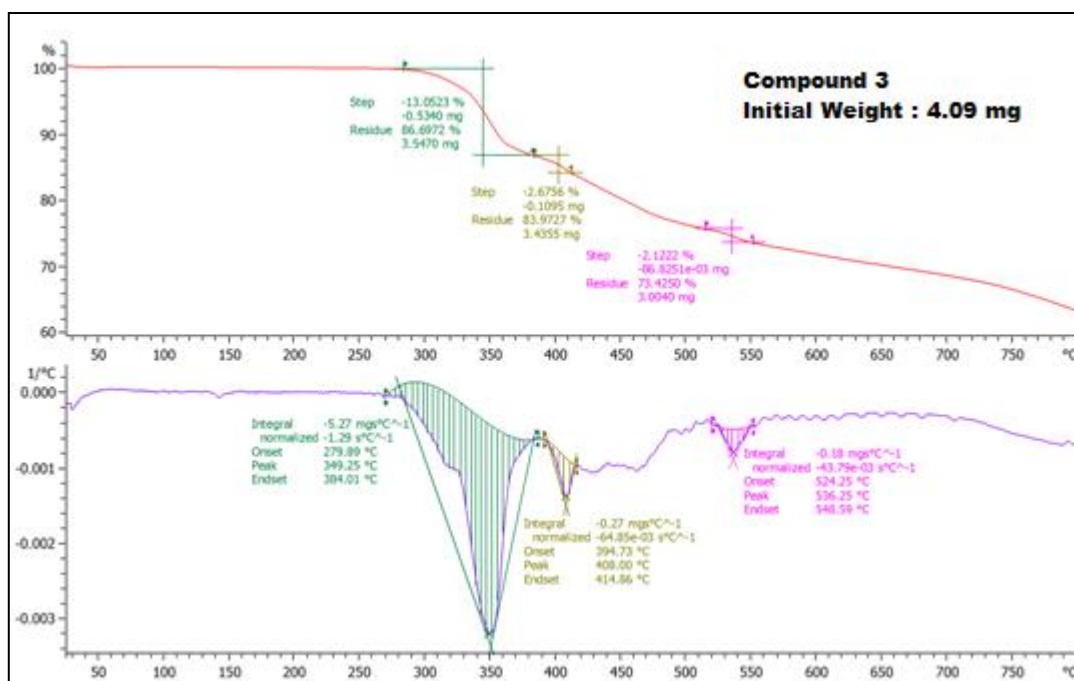


Fig. S10c Thermal analysis plot for compound 3.

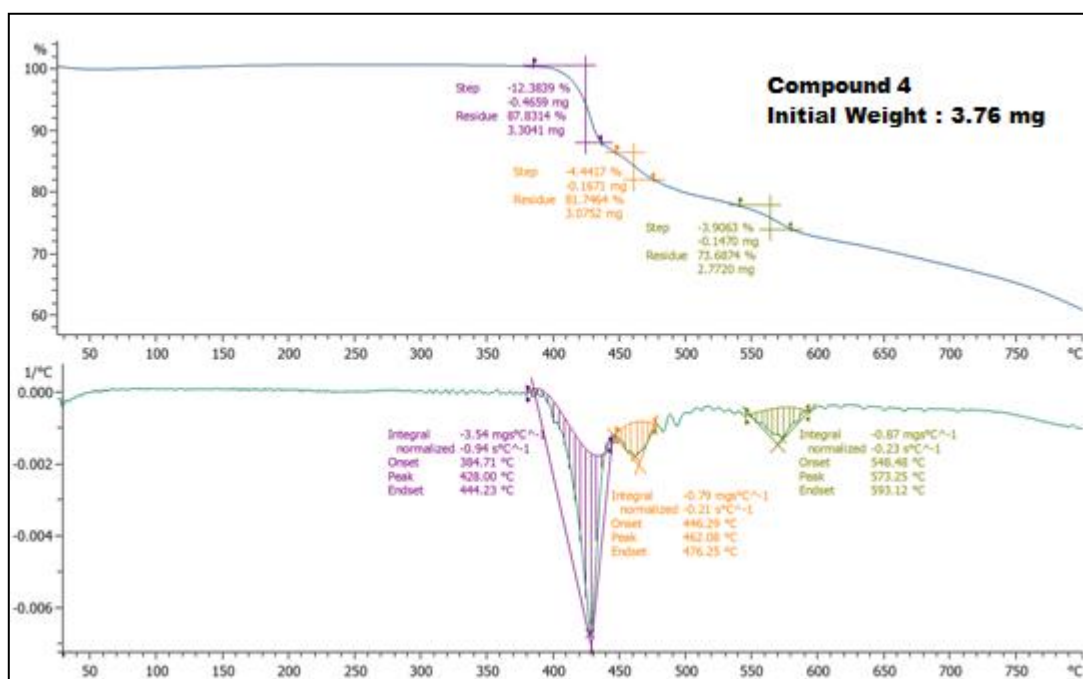


Fig. S10d Thermal analysis plot for compound 4.

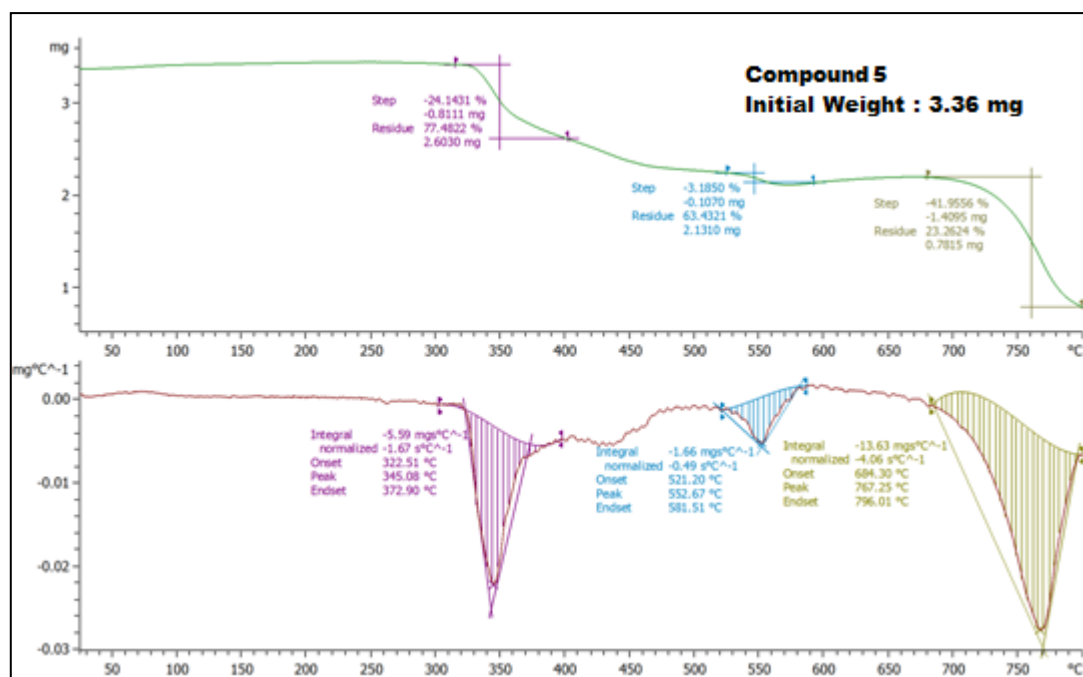


Fig. S10e Thermal analysis plot for compound 5.

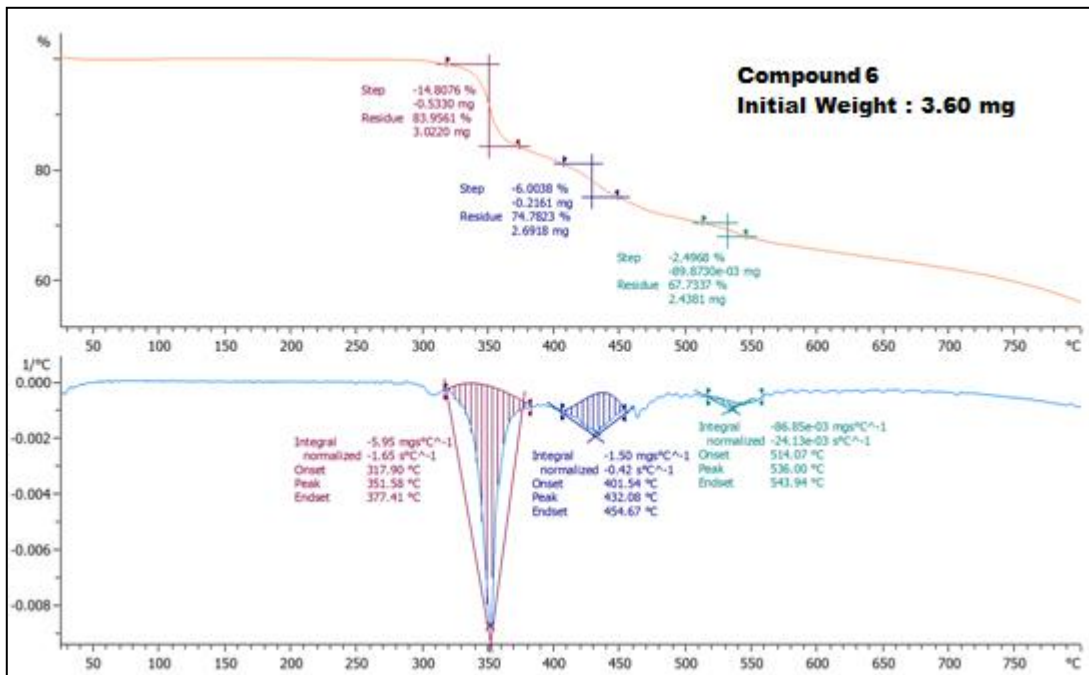


Fig. S10f Thermal analysis plot for compound 6.

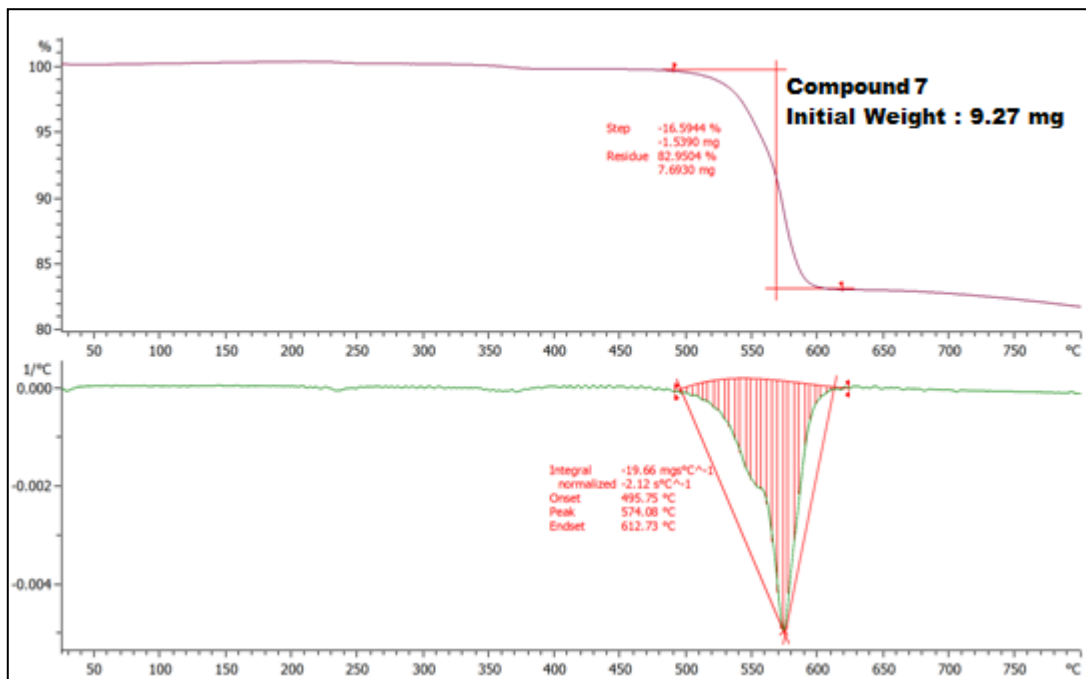


Fig. S10g Thermal analysis plot for compound 7.

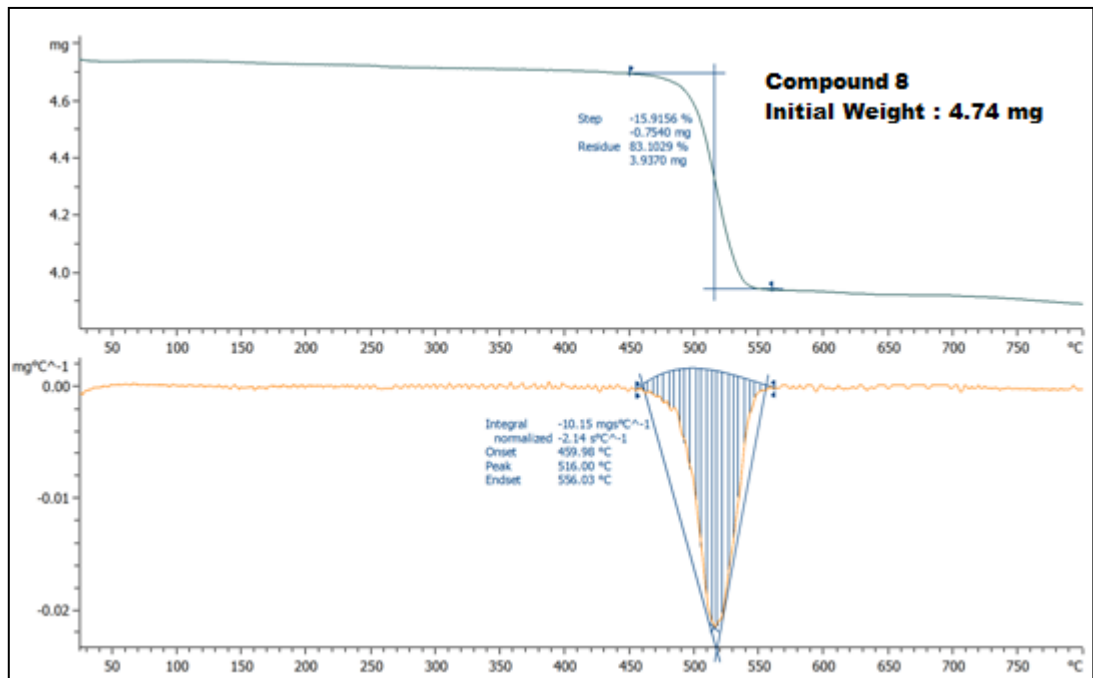


Fig. S10h Thermal analysis plot for compound 8.

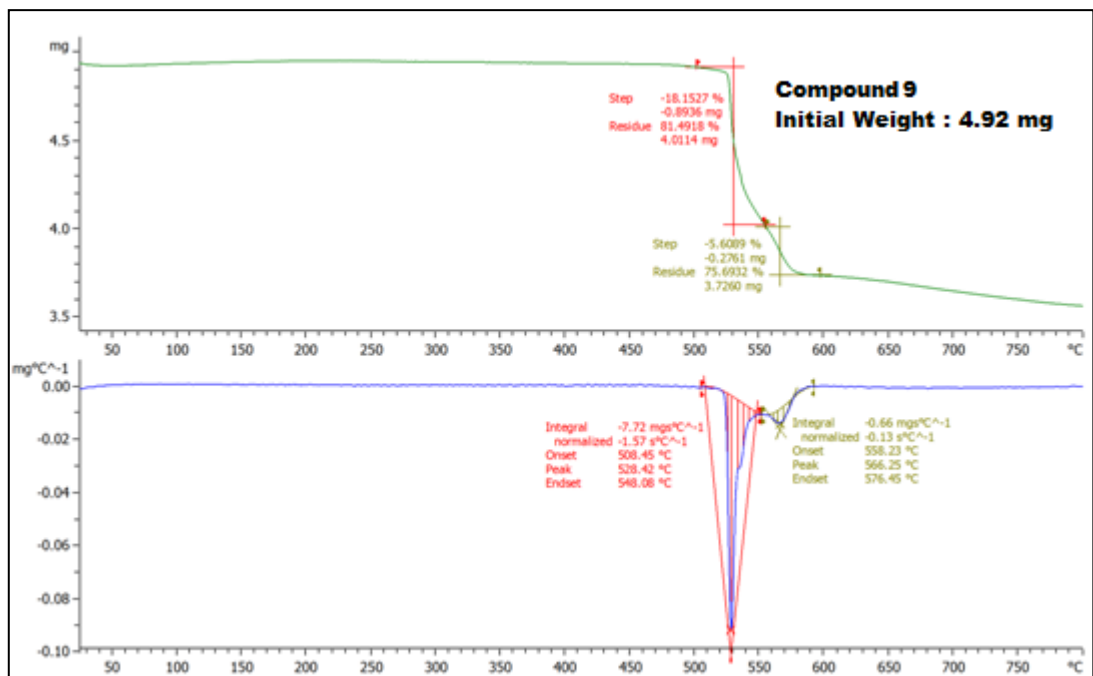


Fig. S10i Thermal analysis plot for compound 9.

S8.2. The thermal analysis for compound **1** exposed to iodine shows a weight loss in the temperature range of 73°-150°C. Since the parent compound shows no weight loss prior to 300°C, the observed weight loss for iodine exposed compound **1** corresponds to the loss of iodine (Fig. S11).

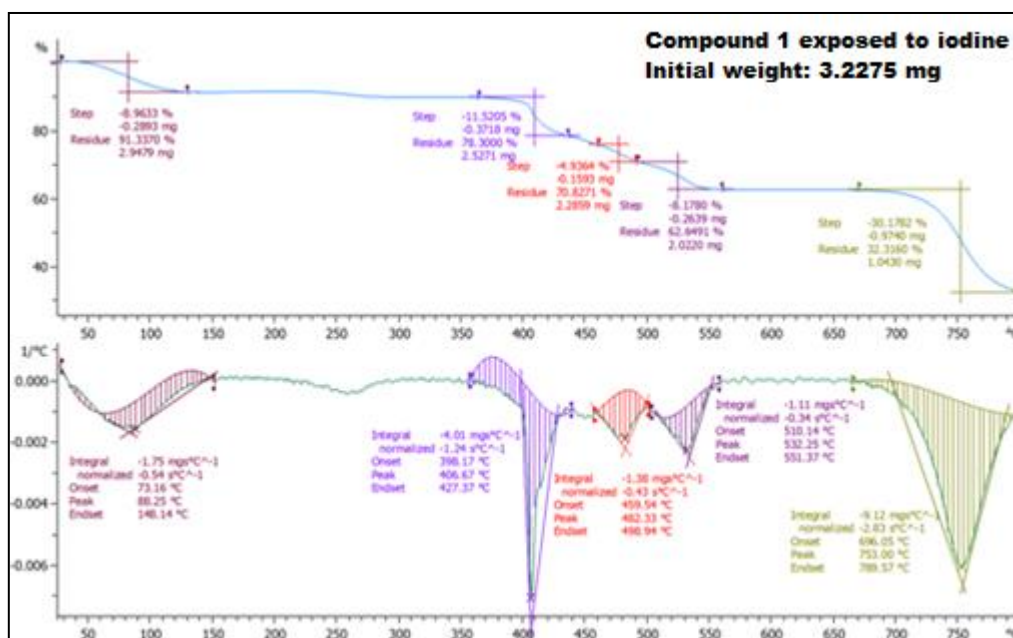


Fig. S11. Thermal analysis plot for compound **1** exposed to iodine.

S8.3. The thermal analysis for compound **1** exposed to CS₂ shows a single step weight loss in the temperature range of 30°-70°C which was not observed for the parent compound **1**. This weight loss can be said to correspond to the loss of CS₂ adsorbed by compound **1** (Fig. S12).

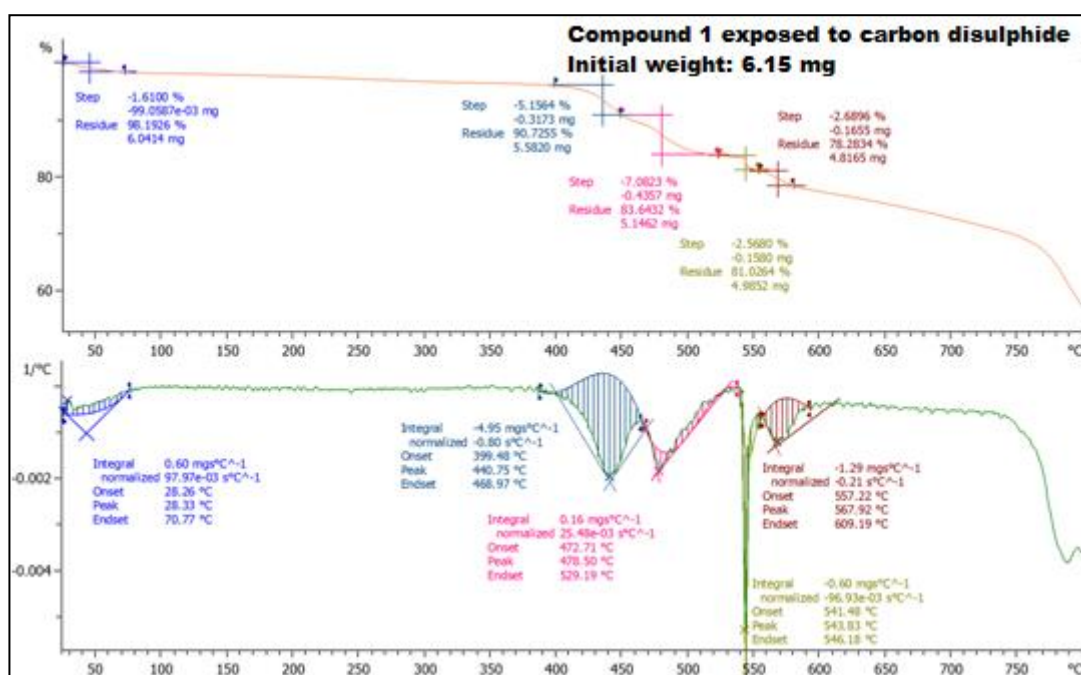


Fig. S12 Thermal analysis plot for compound **1** exposed to CS₂.

Section S9. N₂ Sorption Studies

S9.1. Fig. S13 shows the nitrogen sorption isotherms for compounds 1-9.

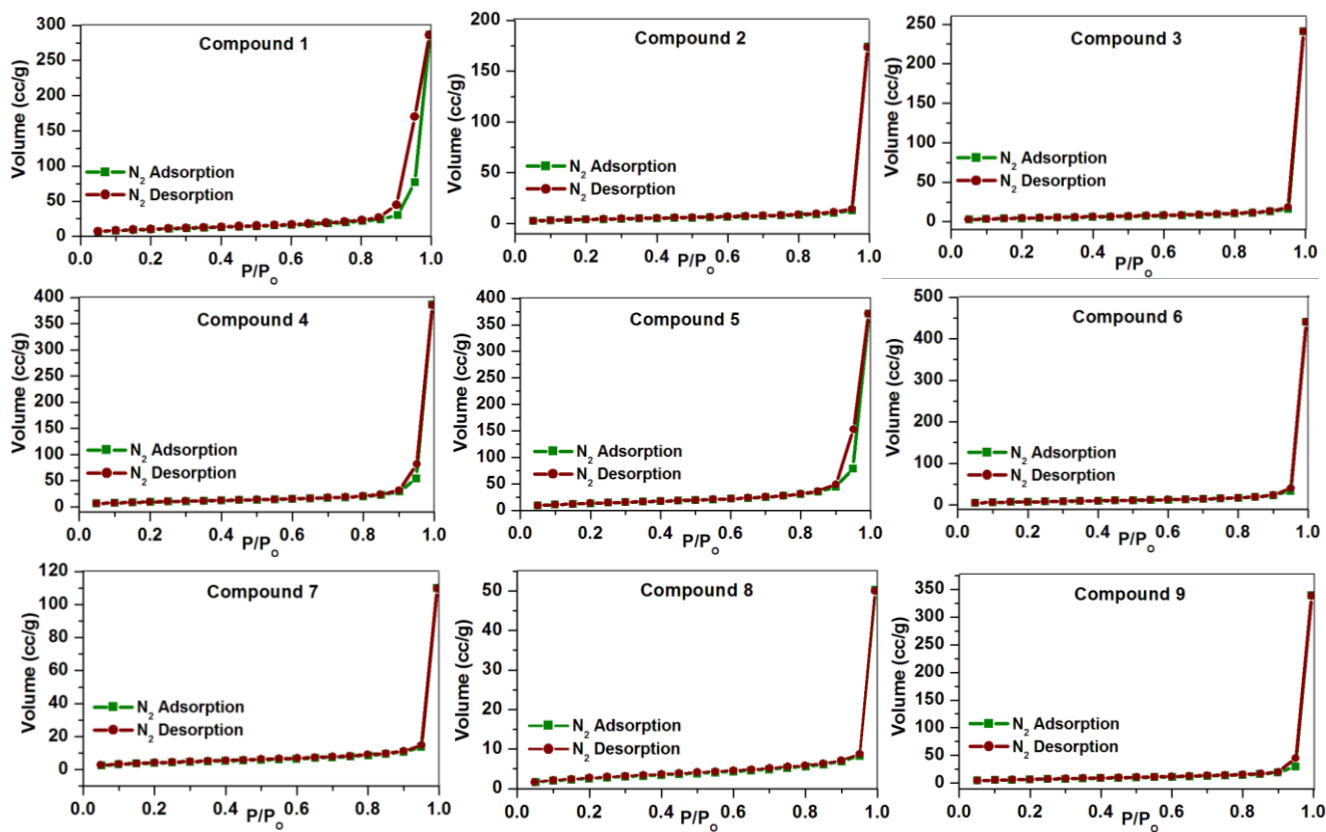


Fig. S13 BET curves for compounds 1-9.

S9.2. The BET surface area, average pore diameter and pore volume of mesoporous compounds **1-9** are summarised in Table S1.

Compound	Surface area (m²/g)	Pore diameter (nm)	Pore volume (cc/g)
Compound 1	36.28	24.3	0.44
Compound 2	14.06	38.3	0.27
Compound 3	16.13	46.2	0.17
Compound 4	34.11	35.0	0.60
Compound 5	47.84	23.2	0.57
Compound 6	27.92	48.3	0.68
Compound 7	14.77	23.2	0.17
Compound 8	9.62	16.14	0.08
Compound 9	25.22	41.5	0.52

Section S10. Iodine (I₂) adsorption by mesoporous compounds 1-9

The amount of iodine adsorbed by compounds **1-9** was determined through the method of linear correlation. This method involved the preparation of iodine solutions of known concentrations in ethanol and hexane. The UV-visible spectra were recorded for these iodine solutions. Calibration curves relating the concentration to absorbance values were then plotted. The amount of iodine adsorbed by the mesoporous compounds was then determined using the calibration curve.

10.1. Iodine extraction in ethanol

10.1.1. Iodine solutions of known concentrations were prepared in ethanol. The UV-visible spectra were recorded for these iodine solutions (Fig. S14).

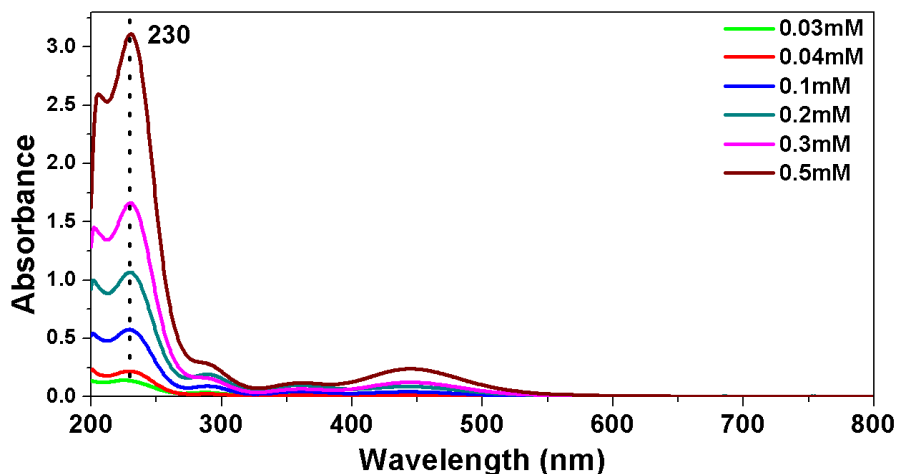
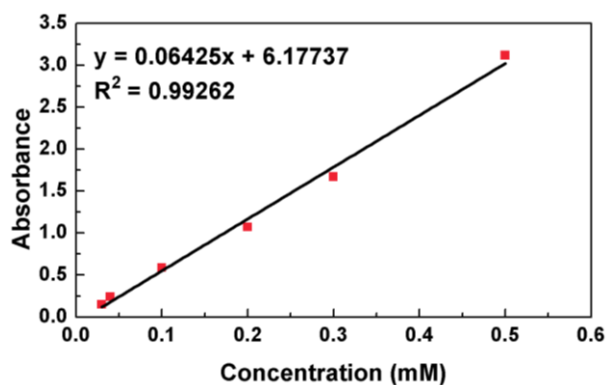


Fig. S14 UV-visible spectra for standard solutions of iodine in ethanol.

10.1.2. Fig. S15 shows the absorbance vs concentration calibration curve for the standard iodine ethanol solutions utilized in the method of linear correlation. Table S2 correlates the absorbance values (at $\lambda = 230$ nm) of the solutions to their known concentration



Concentration of I ₂ solutions in Ethanol (mM)	Absorbance at $\lambda = 230$ nm
0.03	0.147
0.04	0.238
0.10	0.587
0.20	1.070
0.30	1.670
0.50	3.117

Fig. S15. Absorbance vs concentration calibration curve for iodine solutions of known concentrations in ethanol. Table S2. Concentration and corresponding absorbance values of iodine solutions in ethanol.

10.1.3. Compounds **1-9** were exposed to iodine in a gas solid reaction for 15 days. The adsorbed iodine was then extracted in 10 mL ethanol. Table S3 gives the amount of iodine adsorbed by the porous compounds **1-9** by correlating the absorbance values of the ethanol solutions of extracted iodine to their concentration (For the linear correlation method, absorbance values at $\lambda = 230$ nm have been utilized). According to the obtained results, compound **5** shows maximum iodine uptake, adsorbing 1.03 mg of iodine for 1 mg of the compound.

Table S3. Table for the absorbance values of solutions of iodine extracted from compounds **1-9** in ethanol and the related concentration of the iodine solutions.

Compound	Absorbance at $\lambda = 230$ nm	Concentration (mM)	Amount of I₂ adsorbed (mg)	Amount of I₂ adsorbed/mg of substance (mg)
Compound 1	1.093	0.1878	23.83	0.95
Compound 2	0.340	0.0664	8.42	0.34
Compound 3	0.522	0.0969	12.30	0.49
Compound 4	1.133	0.1939	24.61	0.98
Compound 5	1.186	0.2041	25.90	1.03
Compound 6	0.795	0.1421	18.03	0.72
Compound 7	0.464	0.0863	10.95	0.43
Compound 8	0.228	0.0477	6.05	0.24
Compound 9	0.642	0.1142	14.49	0.58

10.1.4. Time dependent iodine adsorption by compound **1** was carried out for 20 days. The adsorbed iodine was extracted in ethanol at certain time intervals and the UV-visible spectra were recorded. Table S4 relates the amount of iodine adsorbed by compound **1** at different intervals of time to the absorbance values observed for the respective ethanol solutions (using method of linear correlation). The amount of iodine adsorbed by **1** showed an increase up to 15 days after which it saturated.

Table S4. Amount of iodine adsorbed by compound **1** at different intervals of time after its extraction in ethanol.

Day	Absorbance	Concentration	Amount of I ₂ adsorbed (mg)	Amount of I ₂ adsorbed/mg of substance (mg)
Day 1	0.341	0.0677	8.59	0.34
Day 3	0.511	0.0956	12.13	0.49
Day 5	0.614	0.1089	13.82	0.55
Day 7	0.639	0.1143	14.51	0.58
Day 10	0.787	0.1394	17.69	0.71
Day 15	1.117	0.1940	24.62	0.98
Day 20	1.218	0.2086	26.47	1.06

10.2. Iodine extraction in hexane

10.2.1. Iodine solutions of known concentrations were prepared in hexane. The UV-visible spectra were recorded for these iodine solutions (Fig. S16).

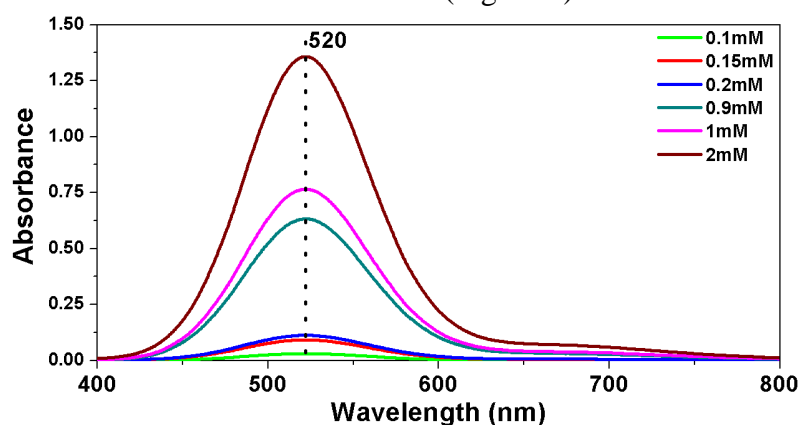


Fig. S16 UV-visible spectra for standard solutions of iodine in hexane.

10.2.2. Fig. S17 shows the absorbance vs concentration calibration curve for hexane solutions of iodine utilized in the method of linear correlation. Table S5 correlates the absorbance values (at $\lambda = 520$ nm) of the solutions to their known concentrations.

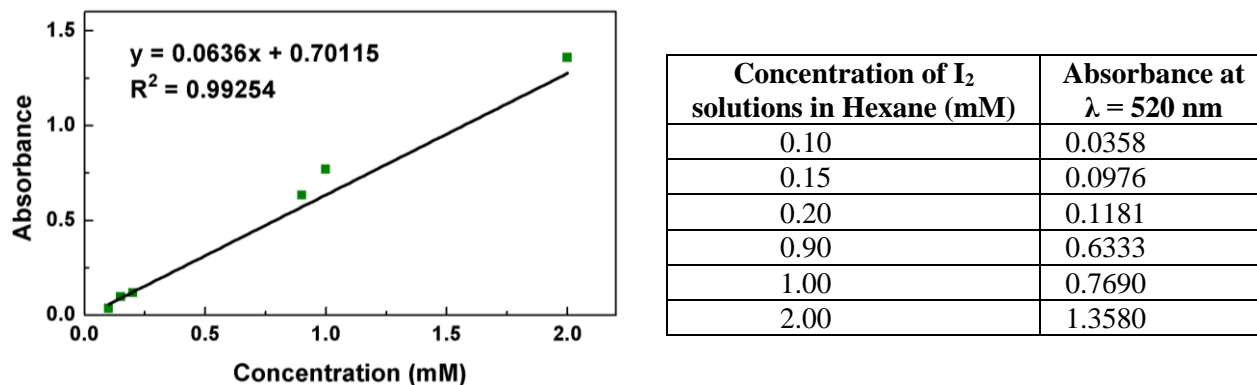


Fig. S17. Absorbance vs concentration calibration curve for iodine solutions of known concentrations in hexane. **Table S5.** Concentration and corresponding absorbance values of iodine solutions in hexane.

10.2.3. Compounds **1-9** were exposed to iodine in a gas solid reaction for 15 days. The adsorbed iodine was then extracted in 10 mL hexane. The UV-visible spectra were recorded for these iodine-hexane solutions (Fig. S18).

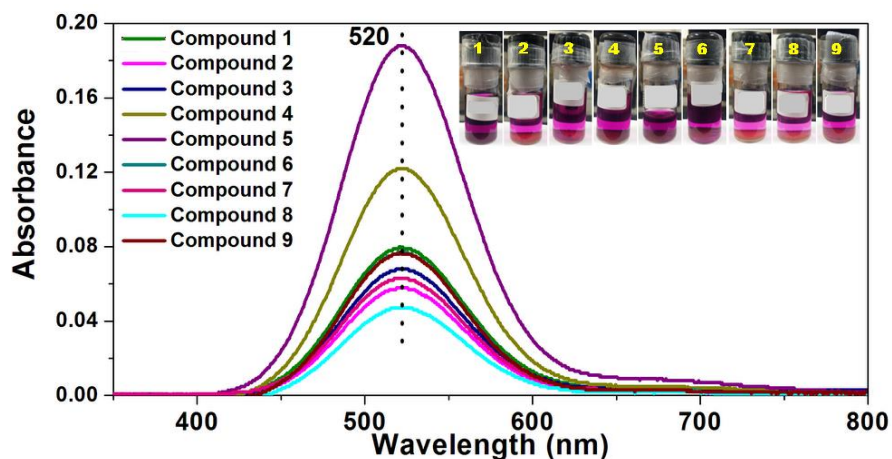


Fig. S18 Solution state UV-Visible spectra for extracted iodine solutions of compounds **1-9** in hexane. The solutions were diluted 50 times prior to recording of the data.

10.2.4. Table S6 gives the amount of iodine adsorbed by the porous compounds **1-9** by correlating the absorbance values of the hexane solutions of extracted iodine to their concentration (For the linear correlation method, absorbance values at $\lambda = 520$ nm have been utilized).

Table S6. Table for the absorbance values of solutions of iodine extracted from compounds **1-9** in hexane and the related concentration of the iodine solutions.

Compound	Absorbance	Concentration	Amount of I ₂ adsorbed (mg)	Amount of I ₂ adsorbed/mg of substance (mg)
Compound 1	0.079	0.1222	15.50	0.82
Compound 2	0.057	0.0824	10.46	0.42
Compound 3	0.068	0.1026	13.02	0.52
Compound 4	0.122	0.1820	23.10	0.92
Compound 5	0.188	0.2768	35.12	1.40
Compound 6	0.077	0.1124	14.26	0.57
Compound 7	0.063	0.0974	12.36	0.49
Compound 8	0.046	0.0675	8.57	0.34
Compound 9	0.076	0.1175	14.91	0.60

10.2.5. Four cycles for the reversible uptake and removal of iodine by compound **1** were performed after every fifteen days. Iodine was extracted in hexane after each cycle of adsorption (Figure S19).

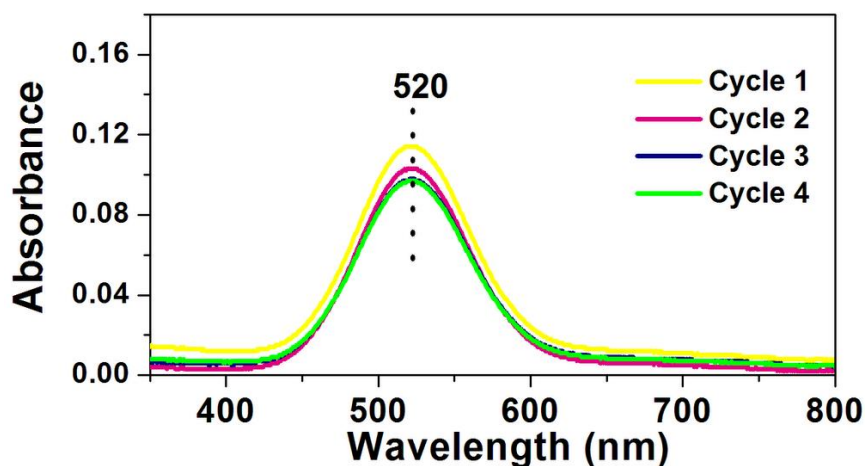


Figure S19. UV-visible spectra for five cycles of reversible uptake of iodine by compound **1**. The adsorbed iodine was extracted in hexane after every cycle.

10.2.6. The amount of iodine adsorbed by compound **1** after every cycle of adsorption is summarized in Table S7.

Table S7. Amount of iodine adsorbed by compound **1** for every reversible cycle of iodine adsorption and desorption.

Cycle	Absorbance	Concentration	Amount of I ₂ adsorbed (mg)	Amount of I ₂ adsorbed/mg of substance (mg)
Cycle 1	0.115	0.1773	22.50	0.90
Cycle 2	0.104	0.1557	19.76	0.79
Cycle 3	0.098	0.1474	18.71	0.75
Cycle 4	0.0970	0.1474	18.71	0.75

10.2.7. Time dependent iodine adsorption by compound **1** was carried out for 20 days. The adsorbed iodine was extracted in hexane at certain time intervals and the UV-visible spectra were recorded. The spectra showed increased adsorption of iodine up till 15 days, after which, it was almost saturated (Fig. S20).

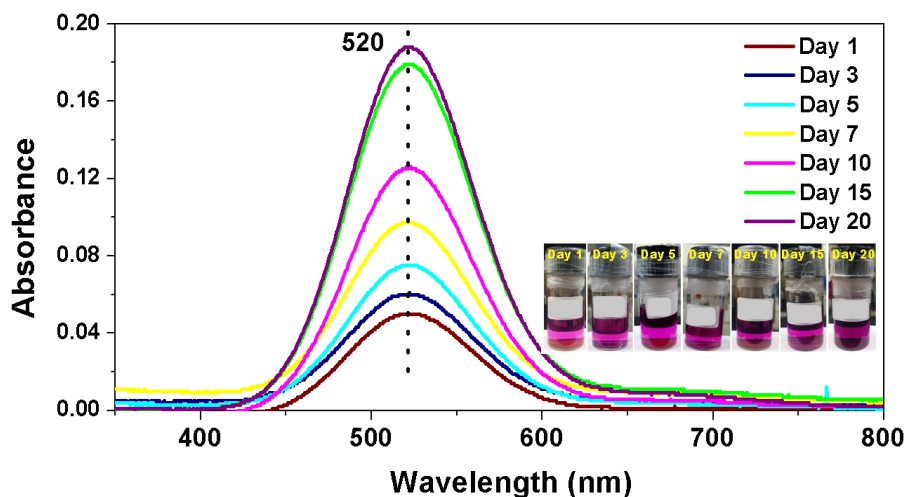


Fig. S20. UV-visible spectra of hexane solutions containing iodine extracted from compound **1** at different intervals of time.

10.2.8. Table S8 relates the amount of iodine, adsorbed by compound **1** at different intervals of time to the absorbance values observed for the respective hexane solutions.

Table S8: Amount of iodine adsorbed by compound **1** at different intervals of time after its extraction in hexane.

Day	Absorbance	Concentration	Amount of I ₂ adsorbed (mg)	Amount of I ₂ adsorbed/mg of substance (mg)
Day 1	0.04	0.0773	9.81	0.39
Day 3	0.0601	0.0876	11.12	0.45
Day 5	0.074	0.1175	14.91	0.60
Day 7	0.098	0.1520	19.29	0.77
Day 10	0.1260	0.1871	23.74	0.95
Day 15	0.1792	0.2685	34.07	1.36
Day 20	0.1881	0.2768	35.12	1.40

Section S11. Adsorption of CS₂ by mesoporous compound **1**

S11.1. The adsorption of CS₂ by mesoporous compound **1** was also confirmed by ¹³C NMR. The ¹³C NMR spectrum recorded for compound **1** exposed to CS₂ vapours showed a peak at δ 193 ppm corresponding to CS₂ (Fig. S21).¹ The other peaks observed were a multiplet solvent

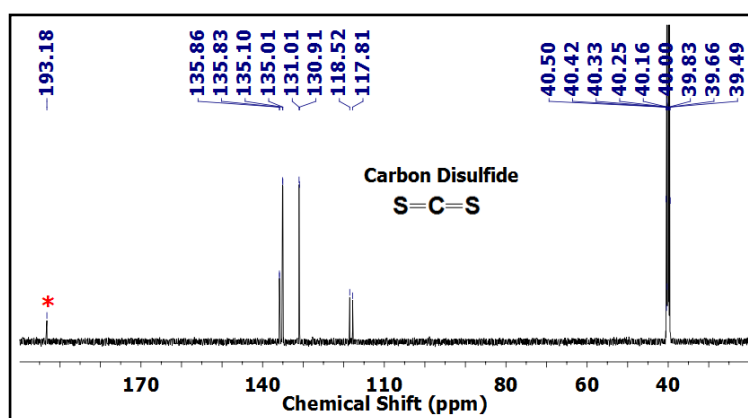


Fig. S21. 125 MHz ¹³C NMR spectrum for compound **1** exposed to CS₂.

peak for d_6 -DMSO at δ 39.5-40.5 ppm and tetraphenylphosphonium cation peaks at δ 117-136 ppm.

S11.2. Three cycles were performed after every seven days for the reversible uptake and removal of CS_2 by compound **1**. The adsorbed CS_2 was leached in methanol after every cycle (Fig. S22).

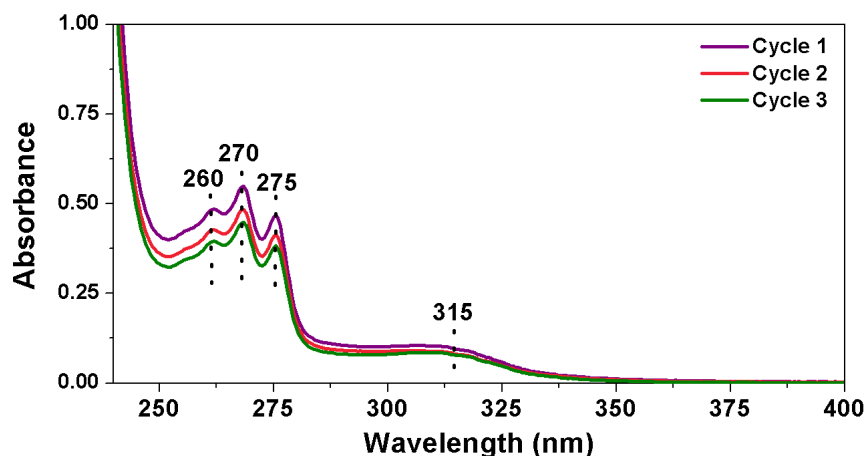


Fig. S22. UV-visible spectra for three cycles of reversible uptake of CS_2 by compound **1**. The adsorbed CS_2 was extracted in methanol after every cycle.

Section S12. Surface potential measurements:

The Atomic force microscopy (AFM) experiments were carried out with oxford instruments and the relevant data were analysed by asylum software. The Kelvin probe force microscopy (KPFM) technique was performed in non-contact mode of operation using conductive probe. The conductive probe was coated with Ti/Ir tip with radius of 25 nm, having a spring constant of 2 N/m and the bias of +3V was applied to the tip.

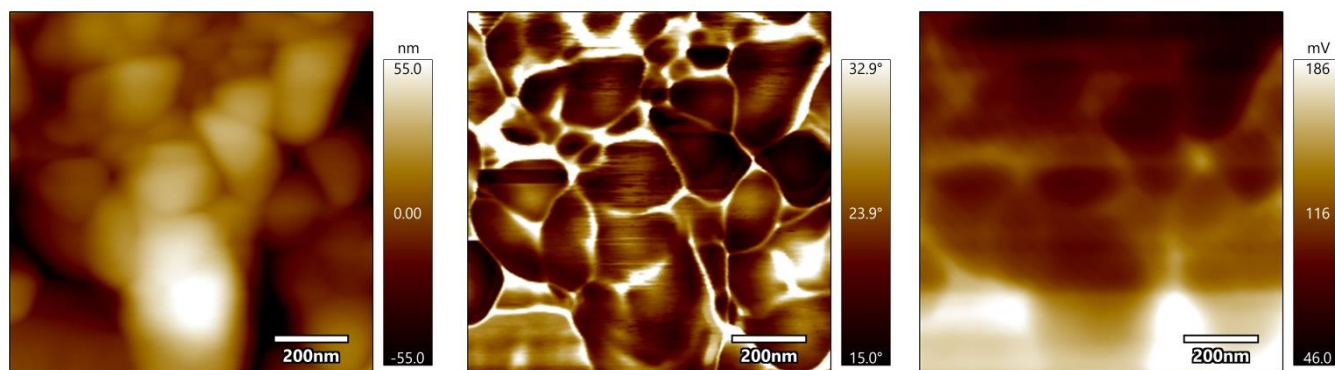


Fig. S23. KPFM images of compound $[PPh_4]_3[PMo_{12}O_{40}]$ (**1**)

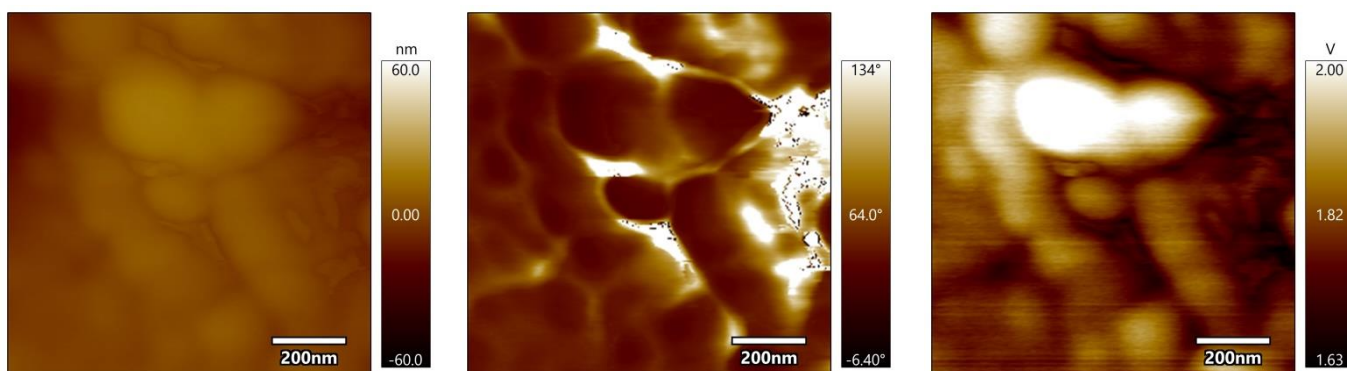


Fig. S24. KPFM images of compound $[\text{EtPPh}_3]_3[\text{PMo}_{12}\text{O}_{40}]$ (**2**)

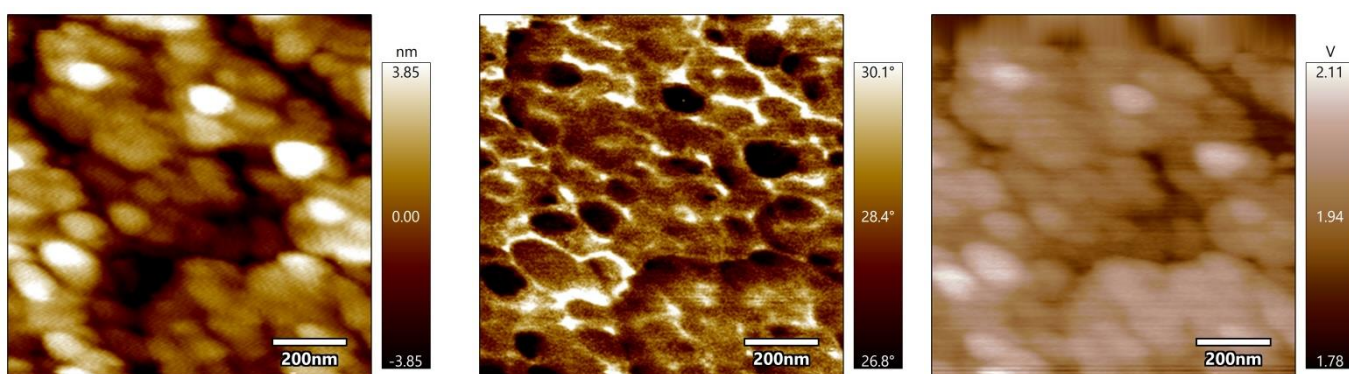


Fig. S25. KPFM images of compound $[\text{PPh}_4]_4[\text{SiMo}_{12}\text{O}_{40}]$ (**4**)

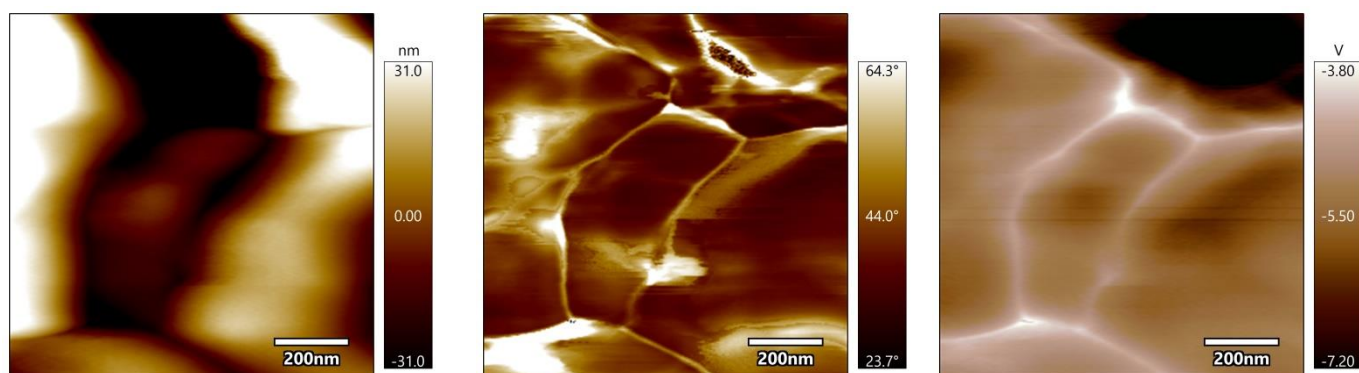


Fig. S26. KPFM images of compound compound $[\text{PPh}_4]_3[\text{PW}_{12}\text{O}_{40}]$ (**7**)

Section S13. Control experiments of iodine adsorption by phosphonium cations

The tetraphenylphosphonium bromide, methyltriphenylphosphonium bromide, ethyltriphenylphosphonium bromide are exposed to iodine vapour. 25 mg of each phosphonium salt of bromide is exposed to iodine vapour for 10 days. The iodine adsorbed phosphonium salts are extracted with hexane in which compound is not soluble. The quantification of the extracted iodine is carried out by UV-Visible spectroscopy monitoring the absorbance at 520nm.

Table S9: Amount of iodine adsorbed by phosphonium salts that are extracted at different intervals of time in hexane.

	Chemical Formula	Hours	Absorbance	Concentration	Amount of I ₂ adsorbed (mg)	Amount of I ₂ adsorbed/mg of substance
1.	[PPh ₄] ₃ Br	3	0.081	0.1275	16.19	0.65
	[PPh ₄] ₃ Br	9	0.107	0.1653	21	0.84
	[PPh ₄] ₃ Br	21	0.116	0.1781	22.61	0.90
	[PPh ₄] ₃ Br	24	0.133	0.2032	25.80	1.03
	[PPh ₄] ₃ Br	96	0.146	0.2211	28.07	1.12
2.	[MePPh ₃] ₄ Br	3	0.121	0.1852	23.52	0.94
	[MePPh ₃] ₄ Br	9	0.132	0.2019	25.64	1.02
	[MePPh ₃] ₄ Br	21	0.137	0.2091	26.55	1.06
	[MePPh ₃] ₄ Br	24	0.142	0.2151	27.31	1.09
	[MePPh ₃] ₄ Br	96	0.153	0.2311	29.34	1.17
3	[EtPPh ₃] ₃ Br	3	0.037	0.0647	8.21	0.32
	[EtPPh ₃] ₃ Br	9	0.045	0.0757	9.61	0.38
	[EtPPh ₃] ₃ Br	21	0.047	0.0797	10.12	0.40
	[EtPPh ₃] ₃ Br	24	0.053	0.0876	11.12	0.44
	[EtPPh ₃] ₃ Br	96	0.094	0.1474	18.71	0.74

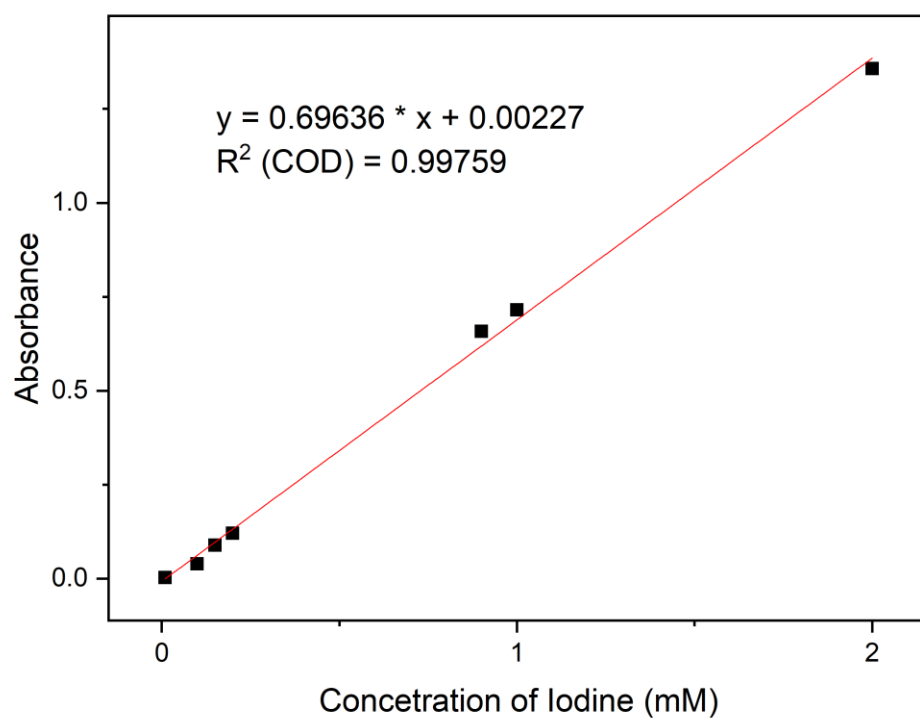


Fig S27. Absorbance vs concentration calibration curve for iodine solutions of known concentrations in hexane.

References

- 1) G. R Fulmer, A. J. M. Miller, N. H. Sherden, H. E. Gottlieb, A. Nudelman, B. M. Stoltz, J. E. Bercaw and K. I. Goldberg, NMR chemical shifts of trace impurities: Common laboratory solvents, organics, and gases in deuterated solvents relevant to the organometallic chemist. *Organometallics*, 2010, **29**, 2176-2179.